

Appendix A: Supplementary Information

Propane Oxidative Dehydrogenation Catalyzed by Molten Metal Alloys

Majd Tabbara¹, Zhiyuan Zong¹, Hugo Dignoes¹, Sarah Chfira^{1,2}, and Chester Upham^{1*}

¹Department of Chemical and Biological Engineering, University of British Columbia, Vancouver, British Columbia, Canada V6T 1Z3

²Université de technologie de Compiègne

* Corresponding author

* E-mail address: chester.upham@ubc.ca

Section 2.1: Molten metal alloy catalyst selection criteria

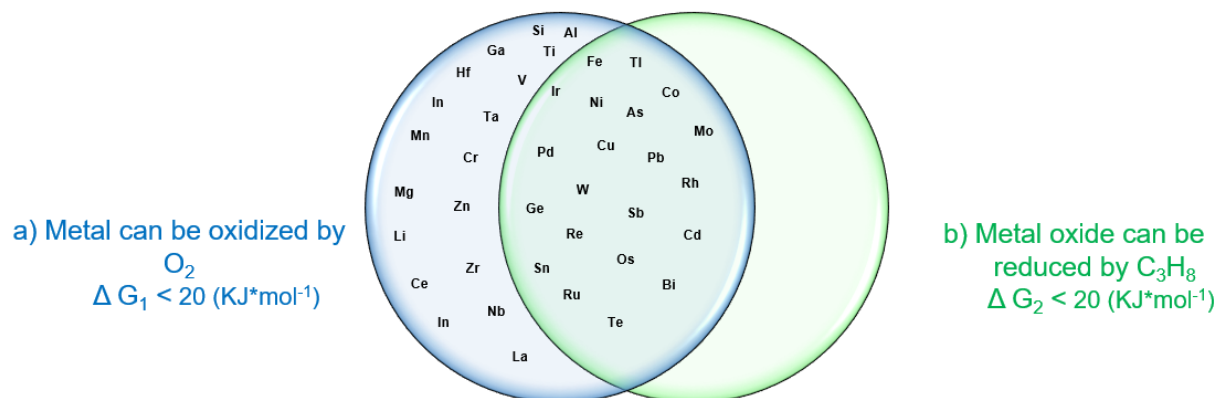


Fig. S-A.1 | Venn diagram representing a summary of thermodynamic properties of eligible metallic candidates for ODH with O_2 as a reactant at $T = 600 \text{ }^\circ\text{C}$ and $P = 1 \text{ atm}$. Notably, the centered metallic candidates do not form a stable metallic carbide

Section 2.2: Catalyst synthesis for screening and overall screening process

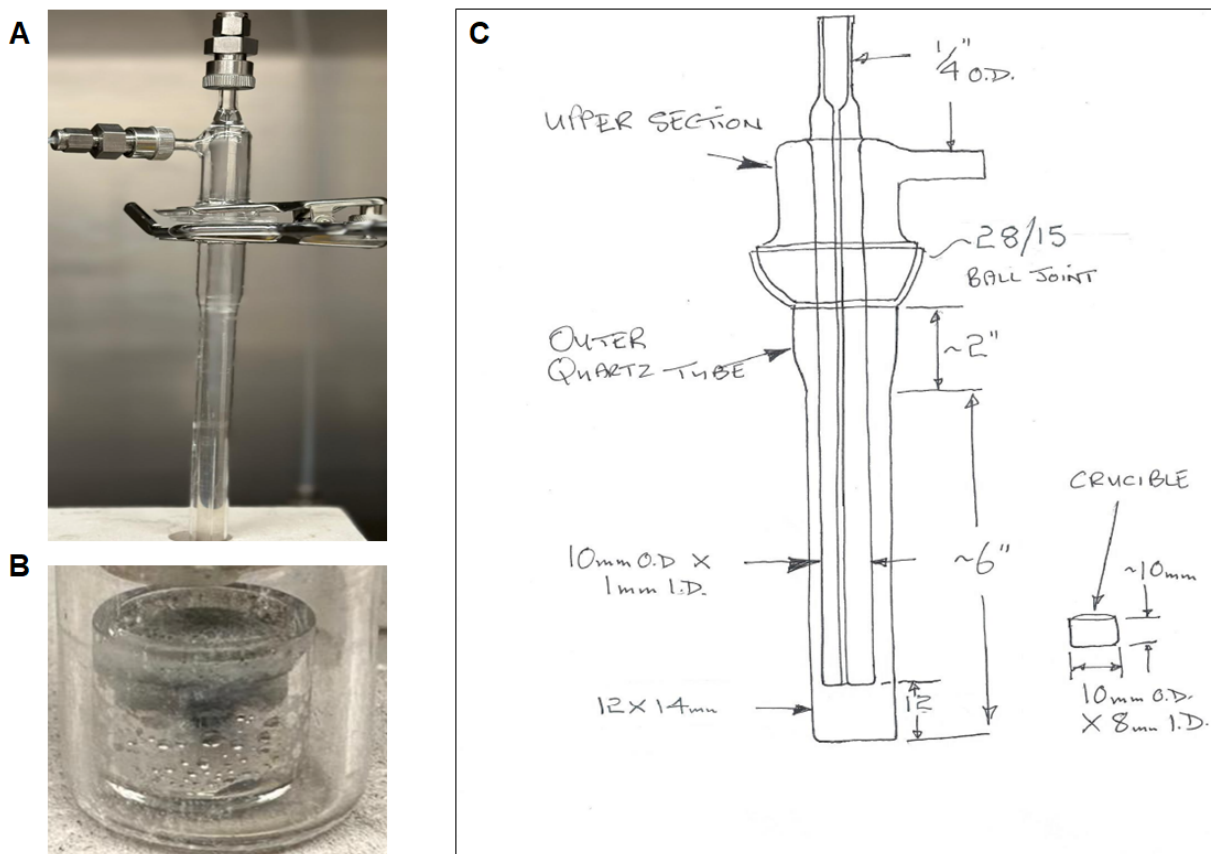


Fig. S-A.2 | A) In-situ experimental depiction of the molten metal catalyst screening reactor at $T = 600\text{ }^{\circ}\text{C}$ and $P = 1\text{ atm}$. **B)** In-situ experimental depiction of an oxide-free molten Bi-Sn alloy within the catalytic screening reactor at $T = 600\text{ }^{\circ}\text{C}$ and $P = 1\text{ atm}$. **C)** Molten metal catalyst screening reactor dimensions inclusive to the molten metal catalyst-containing crucible cup dimensions

Section 2.3: Supported molten catalyst synthesis

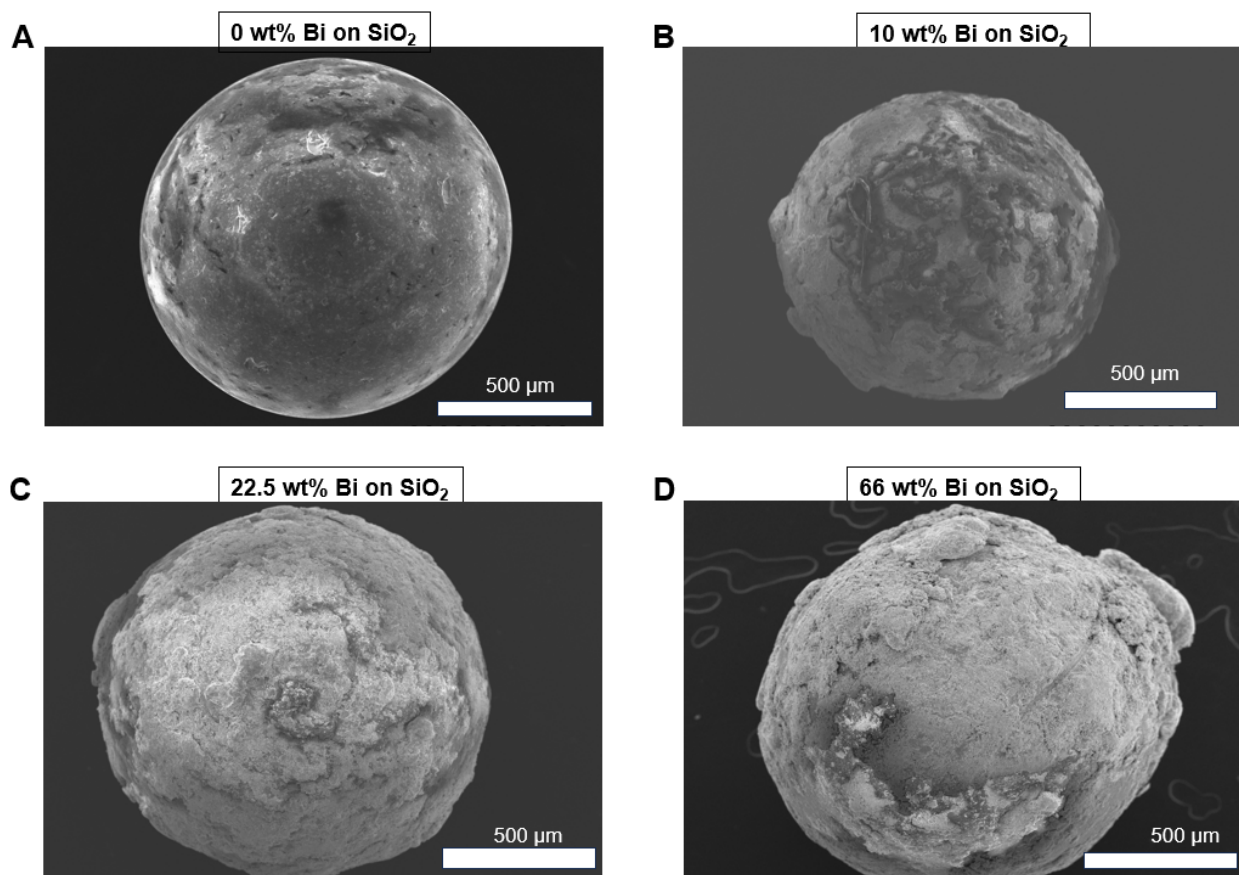


Fig. S-A.3 | SEM images of various borosilicate beads coated with 0-66 wt% Bi. A) 0 wt% Bi coated on a 1 mm bead. **B)** 10 wt% Bi coated on a 1 mm bead. **C)** 22.5 wt% Bi coated on a 1 mm bead. **D)** 66 wt% Bi coated on a 1 mm bead

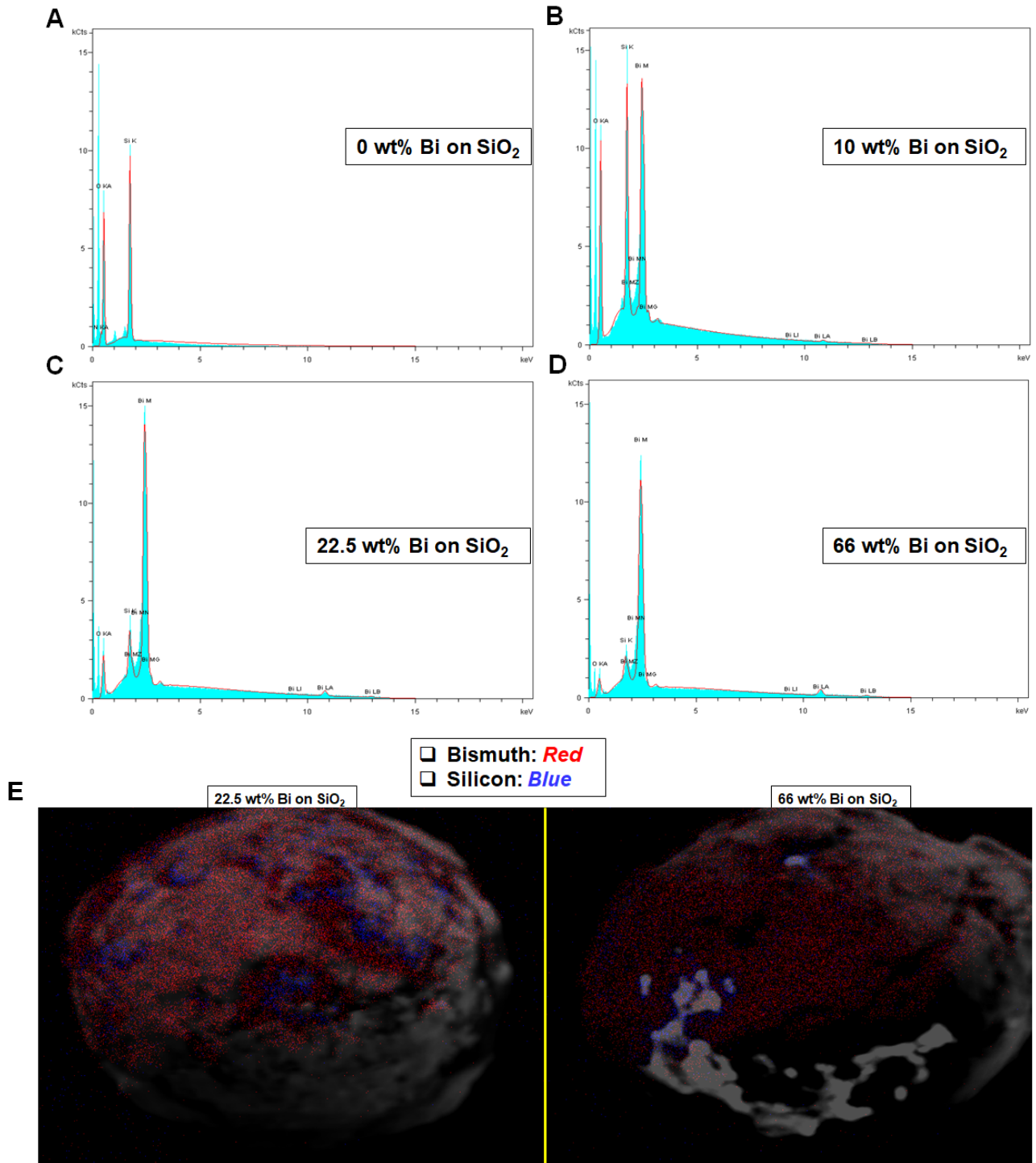


Fig. S-A.4 | EDX spectrums and mapping images of various borosilicate beads coated with 0-66 wt% Bi. A) EDX spectrum for 0 wt% Bi coated on a 1 mm bead. **B)** EDX spectrum for 10 wt% Bi coated on a 1 mm bead. **C)** EDX spectrum for 22.5 wt% Bi coated on a 1 mm bead. **D)** EDX spectrum for 66 wt% Bi coated on a 1 mm bead. **E)** EDX images mapping the surface of 22.5 wt% Bi and 66 wt% Bi on a 1 mm bead

Section 2.5: Reactions on supported liquid metals

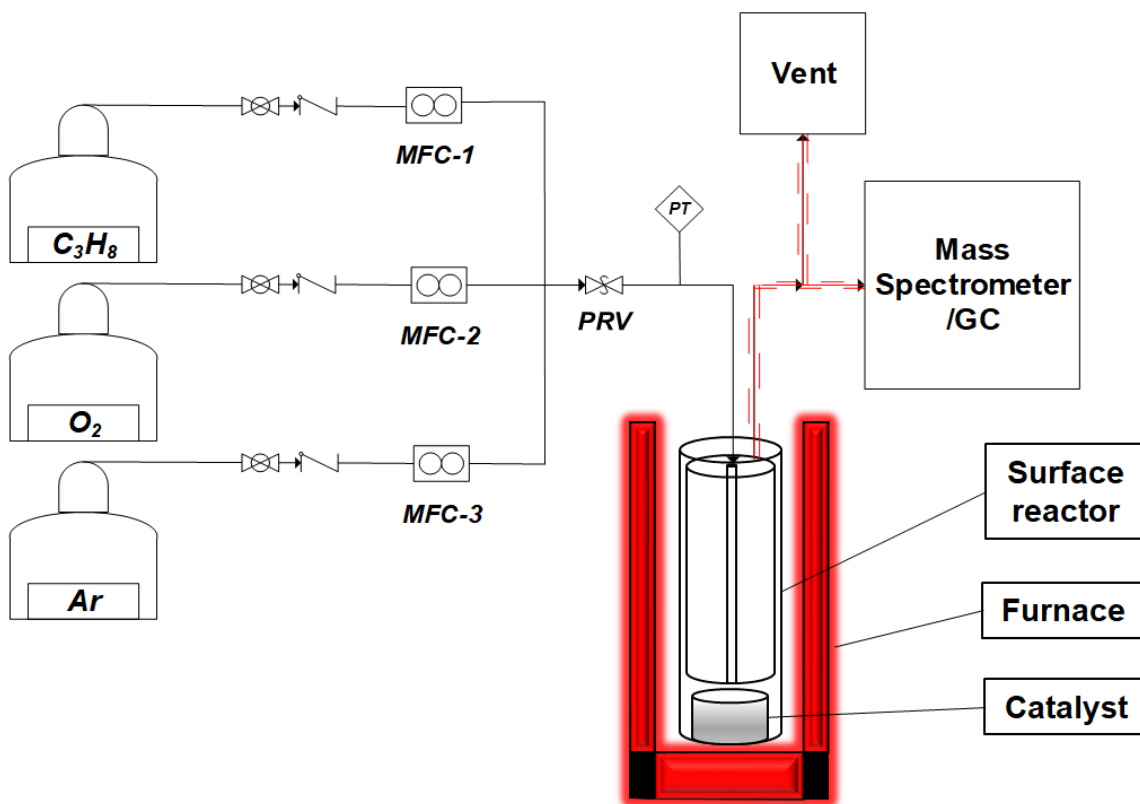


Fig. S-A.5 | Schematic depicting the molten metal catalyst-containing surface reactor. Reactant gases flow over 0.503 cm^2 of molten metal catalyst which is thereafter analyzed via a mass spectrometer and a gas chromatograph. The intrinsic dimensions of both the surface reactor and the catalyst-containing crucibles are vividly depicted in Fig. S-A.2

Section 3.3: Co-feeding C_3H_8 and O_2 over supported Bi-Sn: the effect of temperature

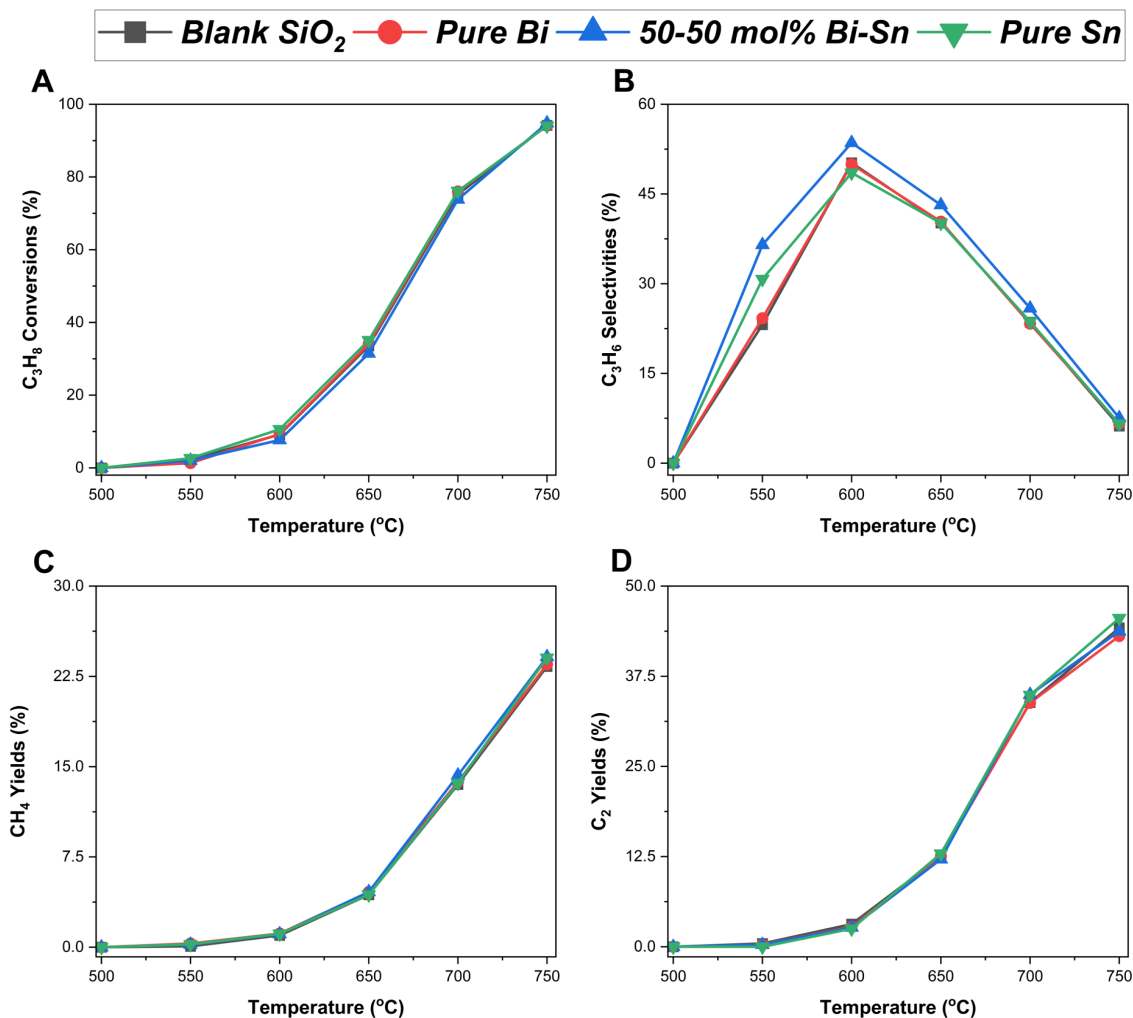


Fig. S-A.6 | Temperature-programmed reaction analyzing the propane dehydrogenation reaction on pure Bi, pure Sn, 50-50 mol% Bi-Sn alloy, and a blank which consists of 3 g borosilicate beads. The analysis was undertaken in a fixed-bed reactor with temperatures ranging from 500-750 °C at 0.29 atm partial pressure of propane in argon (2:7 C_3H_8 :Ar). Performance characteristics were measured and quantified as **A) C_3H_8 conversions, **B)** C_3H_6 selectivities, **C)** CH_4 yields, and **D)** C_2 yields depicted as a function of increasing temperature in the supported liquid metal system**

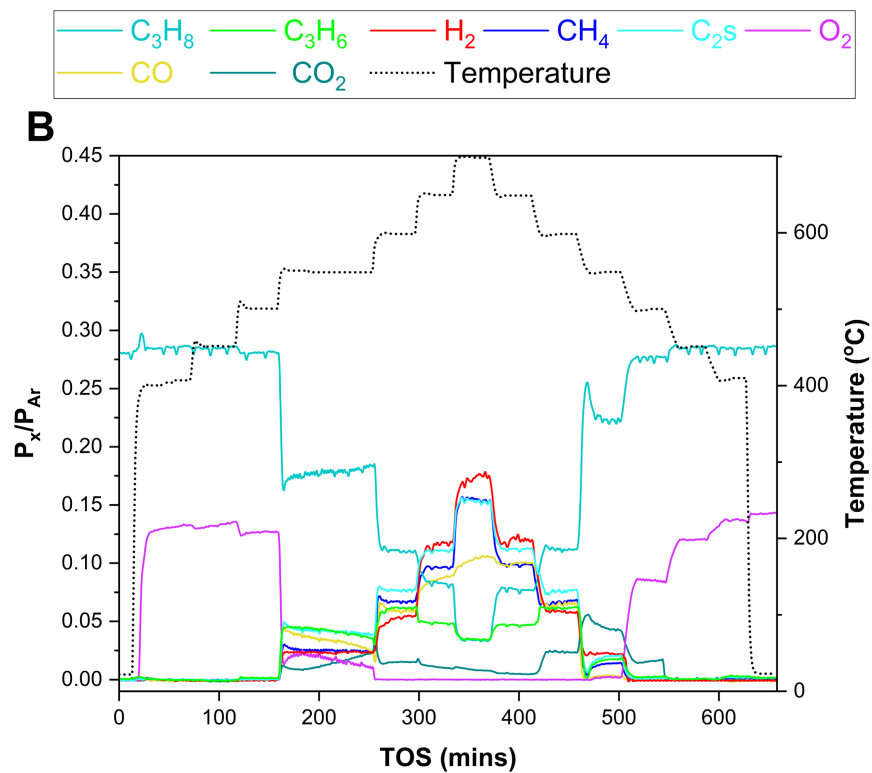
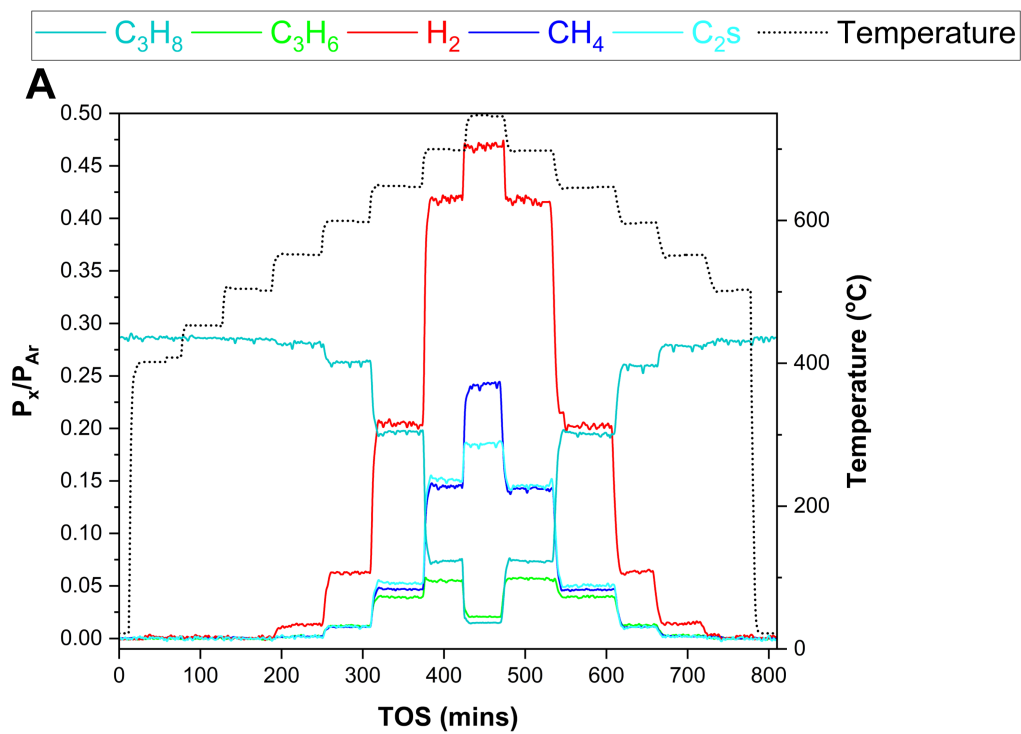


Fig. S-A.7 | Temperature-programmed reaction analyzing propane dehydrogenation and oxidative dehydrogenation on a molten 50-50 mol% Bi-Sn alloy in a fixed-bed reactor. A) The oxygen-free dehydrogenation reaction is illustrated with the partial pressure of propane set at 0.29 atm in argon (2:7 C₃H₈:Ar), and the temperature ranges from 22-750 °C. **B)** The oxidative dehydrogenation reaction is depicted using co-fed oxygen and propane at 0.14 (1:7 O₂:Ar) and 0.29 (2:7 C₃H₈:Ar) atm respectively in argon. Notably, the temperature ranges from 22-700 °C within this analysis

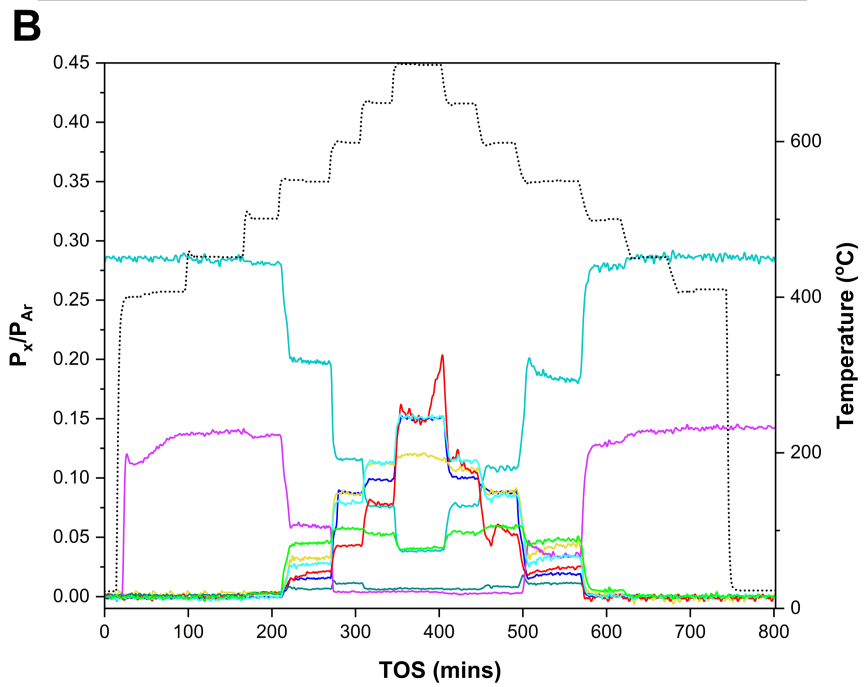
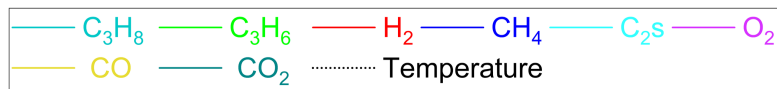
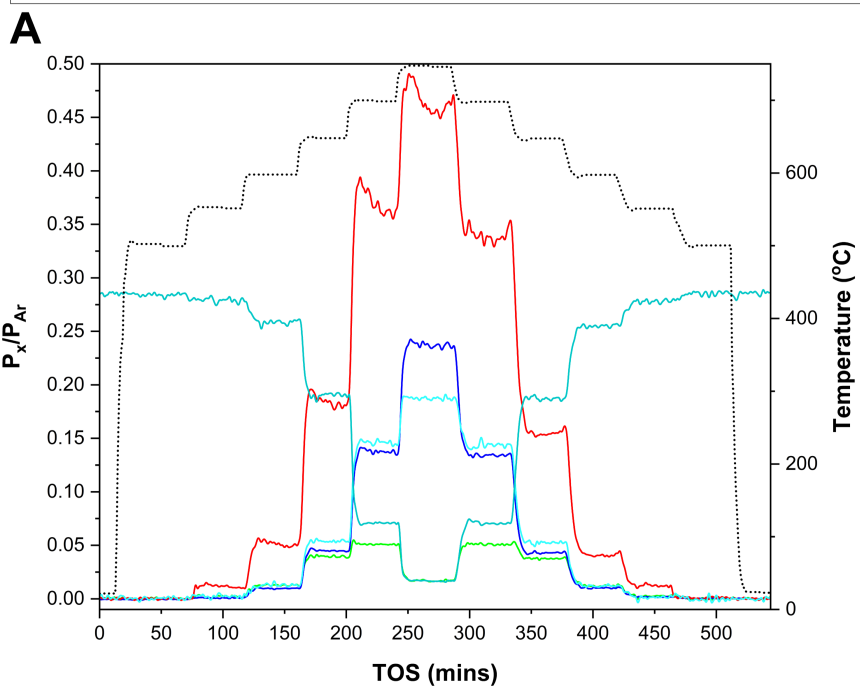
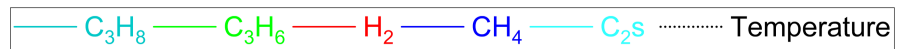


Fig. S-A.8 | Temperature-programmed reaction analyzing propane dehydrogenation and oxidative dehydrogenation on a blank consisting of 3 g borosilicate beads. A) The oxygen-free dehydrogenation reaction is illustrated with the partial pressure of propane set at 0.29 atm in argon (2:7 C₃H₈:Ar), and the temperature ranges from 22-750 °C. **B)** The oxidative dehydrogenation reaction is depicted using co-fed oxygen and propane at 0.14 (1:7 O₂:Ar) and 0.29 (2:7 C₃H₈:Ar) atm respectively in argon. Notably, the temperature ranges from 22-700 °C within this analysis

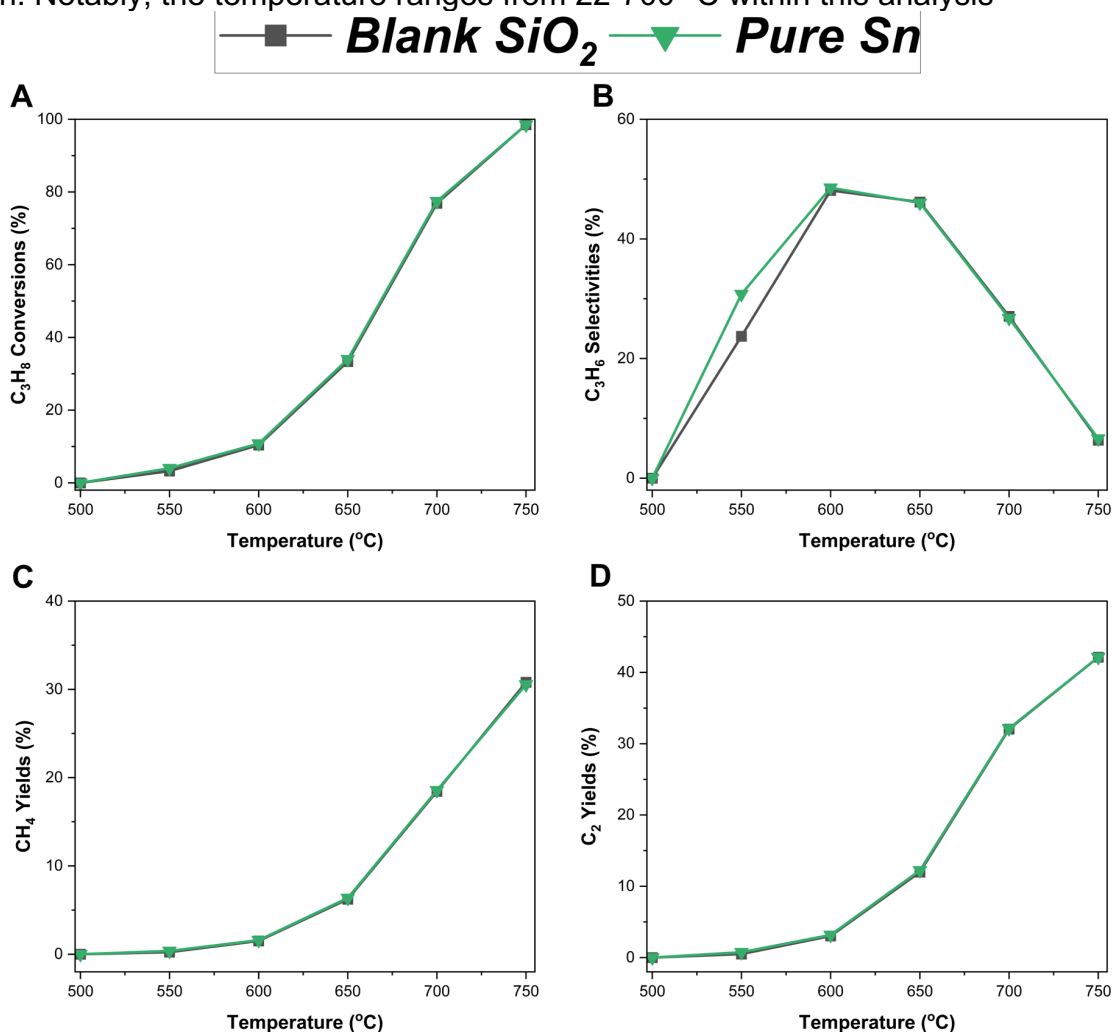


Fig. S-A.9 | Temperature-programmed reaction analyzing the propane dehydrogenation reaction on pure Sn and a blank which consists of 3 g borosilicate beads using the GC. The analysis was undertaken in a fixed-bed reactor with temperatures ranging from 500-750 °C at 0.29 atm partial pressure of propane in argon (2:7 C₃H₈:Ar). Performance characteristics were measured and quantified as **A)** C₃H₈ conversions, **B)** C₃H₆ selectivities, **C)** CH₄ yields, and **D)** C₂ yields depicted as a function of increasing temperature in the supported liquid metal system

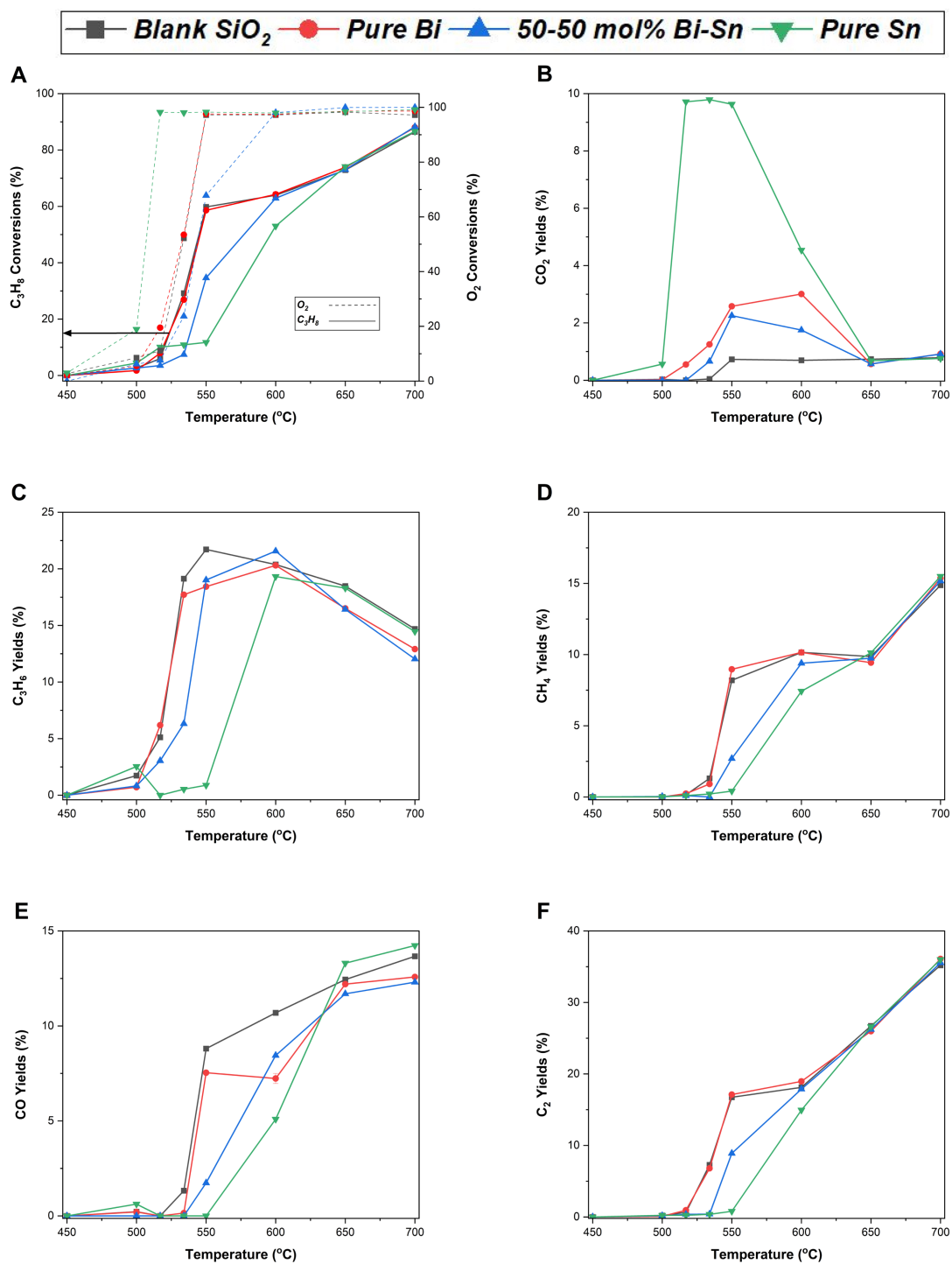


Fig. S-A.10 | Temperature-programmed reaction analyzing the co-fed oxidative dehydrogenation reaction on pure Bi, pure Sn, 50-50 mol% Bi-Sn alloy, and a blank which consists of 3 g borosilicate beads. The analysis was undertaken in a

fixed-bed reactor with temperatures ranging from 450-700 °C at 0.29 atm partial pressure of propane in argon (2:7 C₃H₈:Ar) and 0.14 atm partial pressure of oxygen in argon (1:7 O₂:Ar). Performance characteristics were measured and quantified as **A**) C₃H₈ and O₂ conversions, **B**) CO₂ yields, **C**) C₃H₆ yields, **D**) CH₄ yields, **E**) CO yields, and **F**) C₂ yields depicted as a function of increasing temperature in the supported liquid metal system

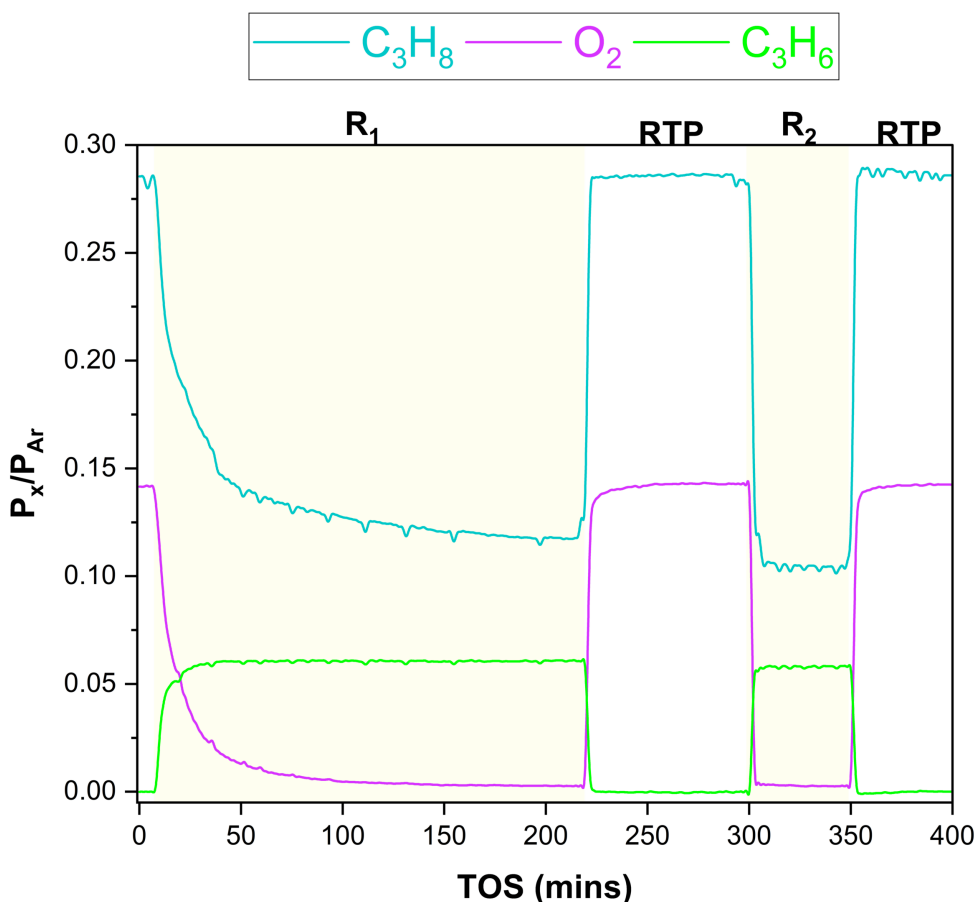


Fig. S-A.11 | Blank 550 °C and 600 °C ODH transients showcasing the longer stabilization period at 550 °C. R₁ and R₂ use an identical partial pressure of oxygen in argon: 0.14 atm (1:7 O₂:Ar). The oxidative dehydrogenation reactions R₁ and R₂ employ 0.29 atm (2:7 C₃H₈:Ar) partial pressure of propane in argon at 550 °C and 600 °C respectively. R₂ was not employed immediately following R₁; instead, it was conducted separately in a fresh reactor to avoid the carryover of coke. The RTP section consists of the reactant gases flowing in Ar (2:1:7 C₃H₈:O₂:Ar) at room temperature and pressure. Note: all blanks consists of 3 g borosilicate beads

Section 3.4.2: Effect of Bi-Sn ratio when cycling between C_3H_8 and O_2

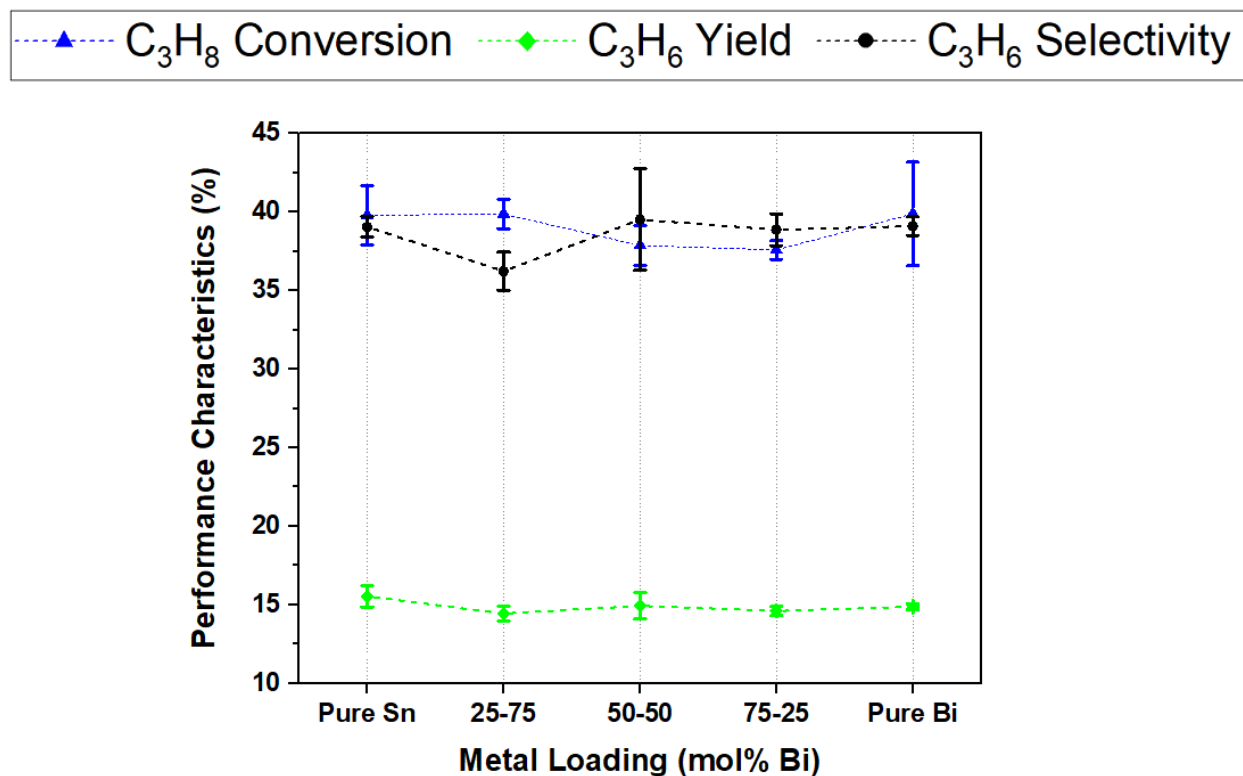


Fig. S-A.12 | Conversion, selectivity, and yield as a function of mol% Bi when C_3H_8 is fed over an oxidized catalyst at 650 °C and 0.29 atm partial pressure of C_3H_8 (2:7 C_3H_8 :Ar). The partial pressure of oxygen in argon during the pre-oxidation was 0.14 atm (1:7 O_2 :Ar). Error bars represent the standard deviation from the mean across three trials

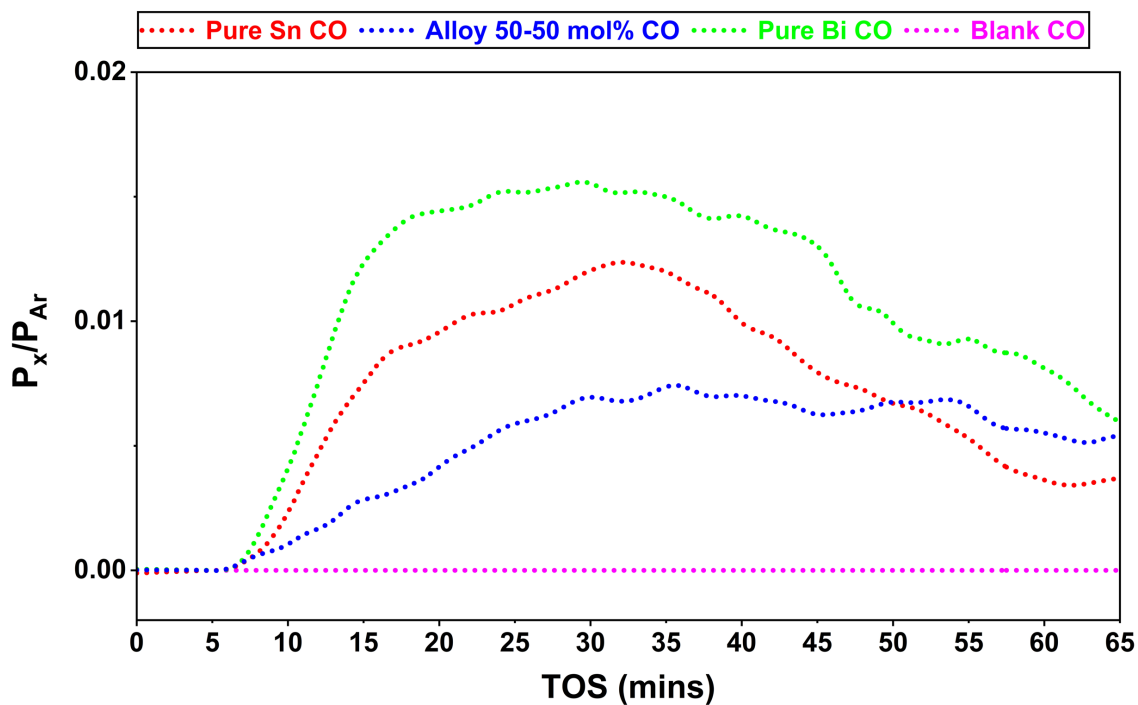


Fig. S-A.13 | CO partial pressures as a function of time on stream over supported catalysts. The melts are reduced at 0.29 atm partial pressure of C_3H_8 at a temperature of 600 °C

Section 3.4.3: Effect of partial pressure, space time, and degree of oxidation

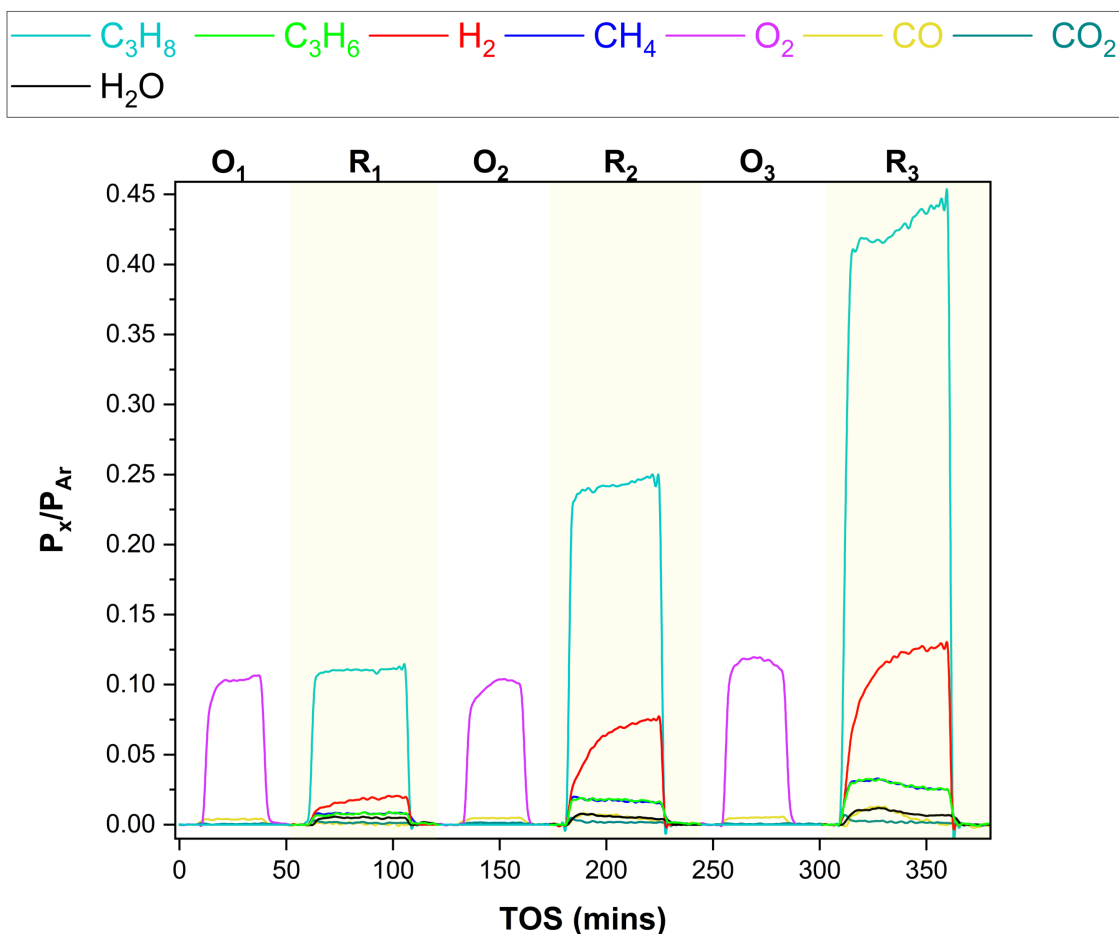


Fig. S-A.14 | Partial pressure optimizations illustrated as a function of increasing partial pressure within the supported molten Bi-Sn system. O₁, O₂, and O₃ use an identical partial pressure of oxygen in argon: 0.14 atm for 30 mins (1:7 O₂:Ar) at 600 °C. The oxidative dehydrogenation reaction R₁ employs 0.13 atm (1:8 C₃H₈:Ar) partial pressure of propane in argon, R₂ utilizes a partial pressure of 0.29 atm (2:7 C₃H₈:Ar), and R₃ implements a partial pressure of 0.5 atm (3:6 C₃H₈:Ar). Argon gas is employed to purge the system in between the optimization steps. Note: all the oxidative dehydrogenation reactions are undertaken at 600 °C

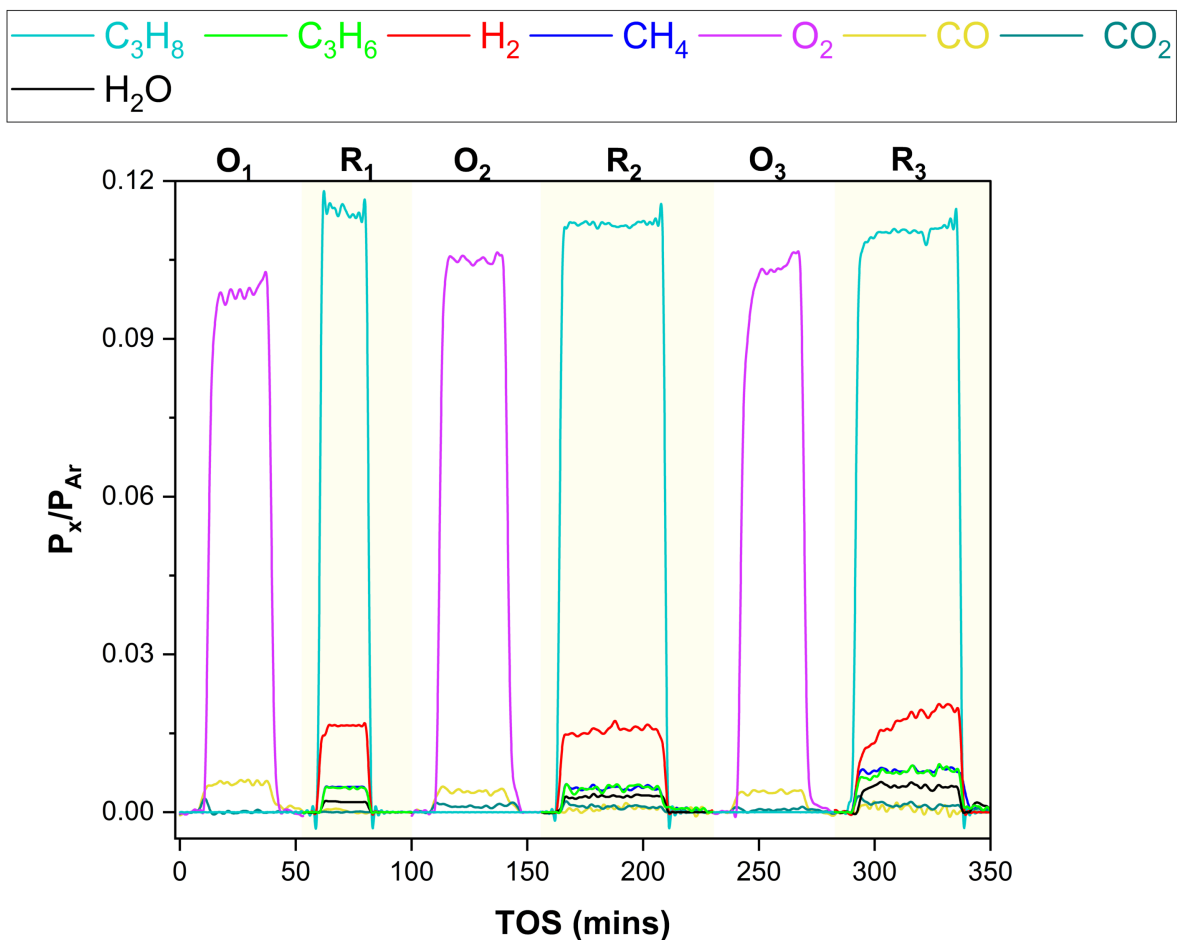


Fig. S-A.15 | Residence time optimizations illustrated as a function of increasing residence time within the supported molten Bi-Sn system. O_1 , O_2 , and O_3 use an identical partial pressure of oxygen in argon: 0.14 atm for 30 mins (1:7 O_2 :Ar) at 600 °C. The oxidative dehydrogenation reaction R_1 , R_2 , and R_3 employ a similar partial pressure of 0.13 atm (1:8 C_3H_8 :Ar) at 600 °C. R_1 , R_2 , and R_3 have a total flowrate of 27, 13.5, and $9 \frac{mL}{min}$ respectively within this analysis. Similarly, argon gas is employed to purge the system in between the optimization steps

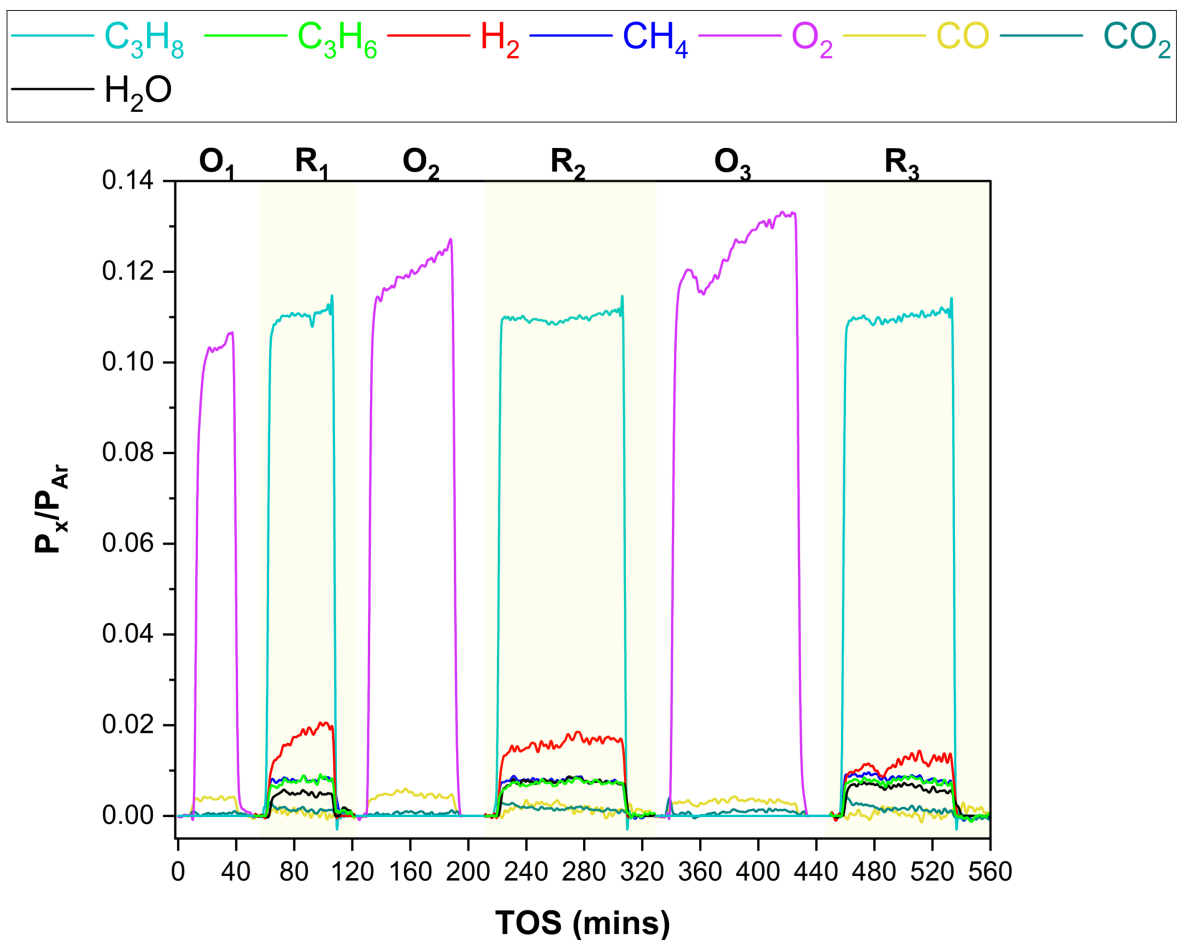


Fig. S-A.16 | Oxide length optimizations illustrated as a function of increasing oxidation pulses within the supported molten Bi-Sn system. The oxidative dehydrogenation reaction R₁, R₂, and R₃ employ an identical partial pressure of 0.13 atm (1:8 C₃H₈:Ar) at 600 °C. O₁, O₂, and O₃ use an identical partial pressure of 0.14 atm (1:7 O₂:Ar) at 600 °C. Respectively, the oxide pulse length is 30, 60, and 90 mins for O₁, O₂, and O₃. Argon gas is employed to purge the system in between the optimization steps

Section 3.6: Supported Bi-Sn and post-reaction characterization

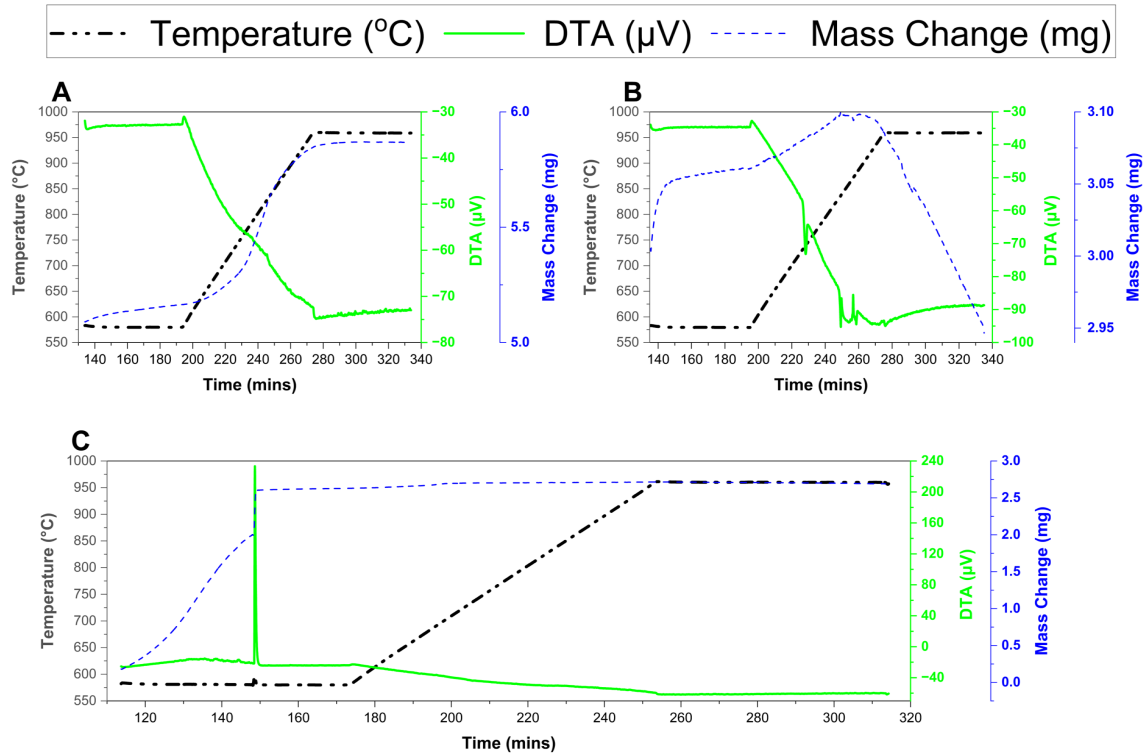


Fig. S-A.17 | TGA results for pure Sn, pure Bi, and a 50-50 mol% Bi-Sn alloy as a function of increasing temperature from 580-960 °C. A) Pure Sn, B) pure Bi, and C) 50-50 mol% Bi-Sn alloy are illustrated in the figure. All metals of interest are oxidized in an inert atmosphere with an hour hold time at 580 and 960 °C

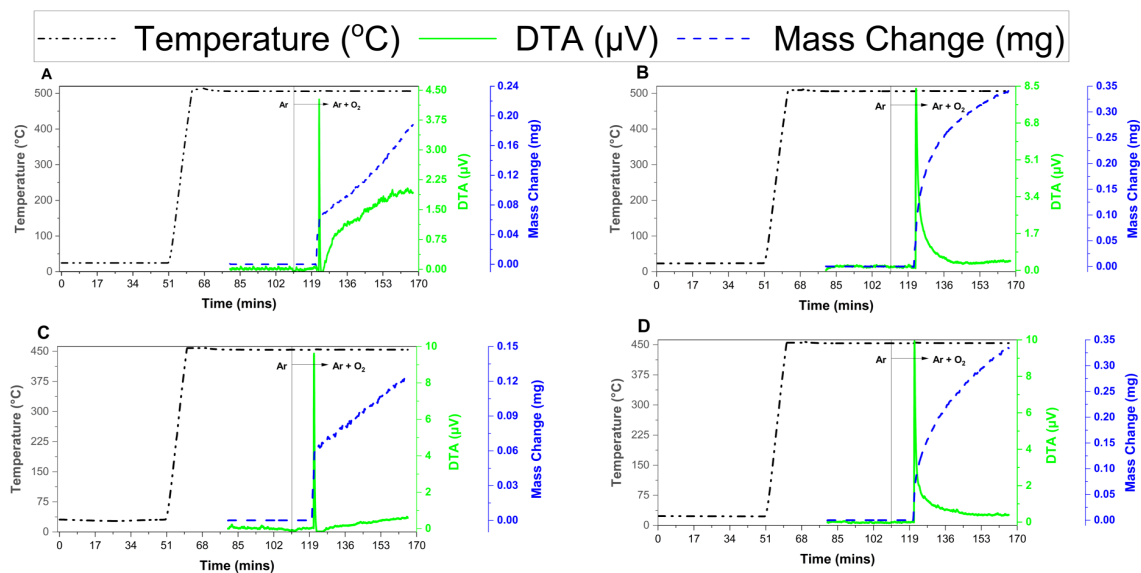


Fig. S-A.18 | TGA results for pure Sn and pure Bi at 450 and 500 °C. A) Pure Sn at 500 °C with initial mass of 20.5 mg, **B)** pure Bi at 500 °C with initial mass of 20.7 mg, **C)** pure Sn at 450 °C with initial mass of 20.7 mg, and pure Bi at 450 °C with initial mass of 20.7 mg

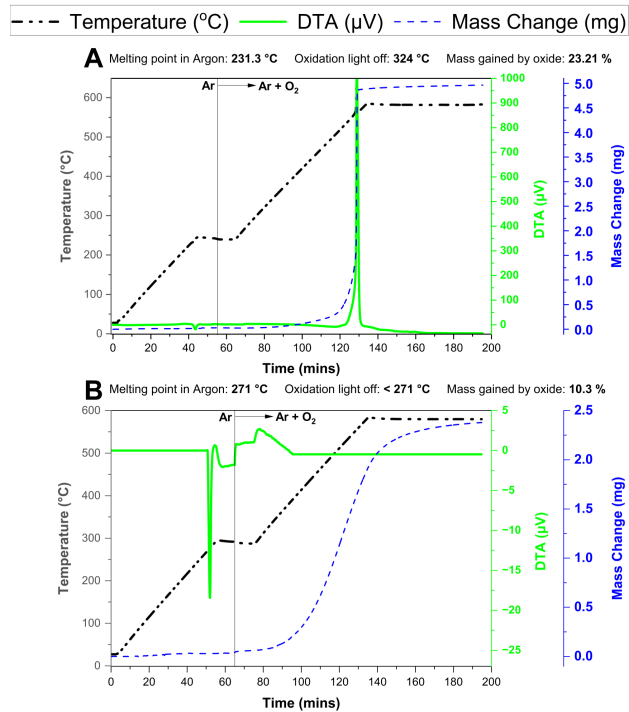


Fig. S-A.19 | TGA replicates for pure Sn and pure Bi. A) Pure Sn and B) pure Bi.
 Note: conditions are identical to the runs depicted in Figure 10

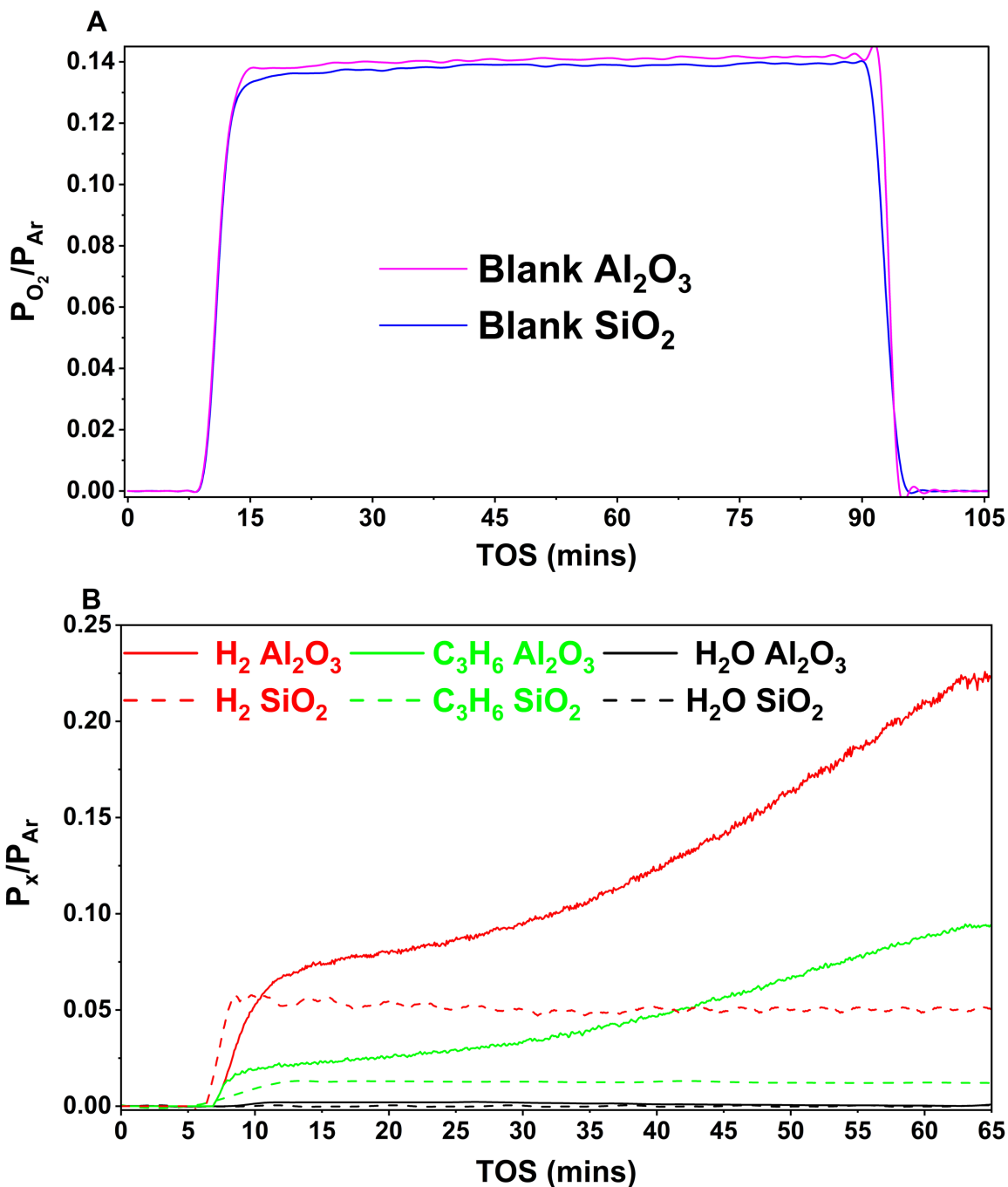


Fig. S-A.20 | Comparison of blank alumina to borosilicate using 3 g Al_2O_3 spheres with 0.28 g glass wool. A) The spheres are oxidized at 0.14 atm partial pressure of oxygen in argon prior to the dehydrogenation reaction. **B)** The spheres are reduced at 0.29 atm partial pressure of C_3H_8 . Temperature is 600 °C in both cases

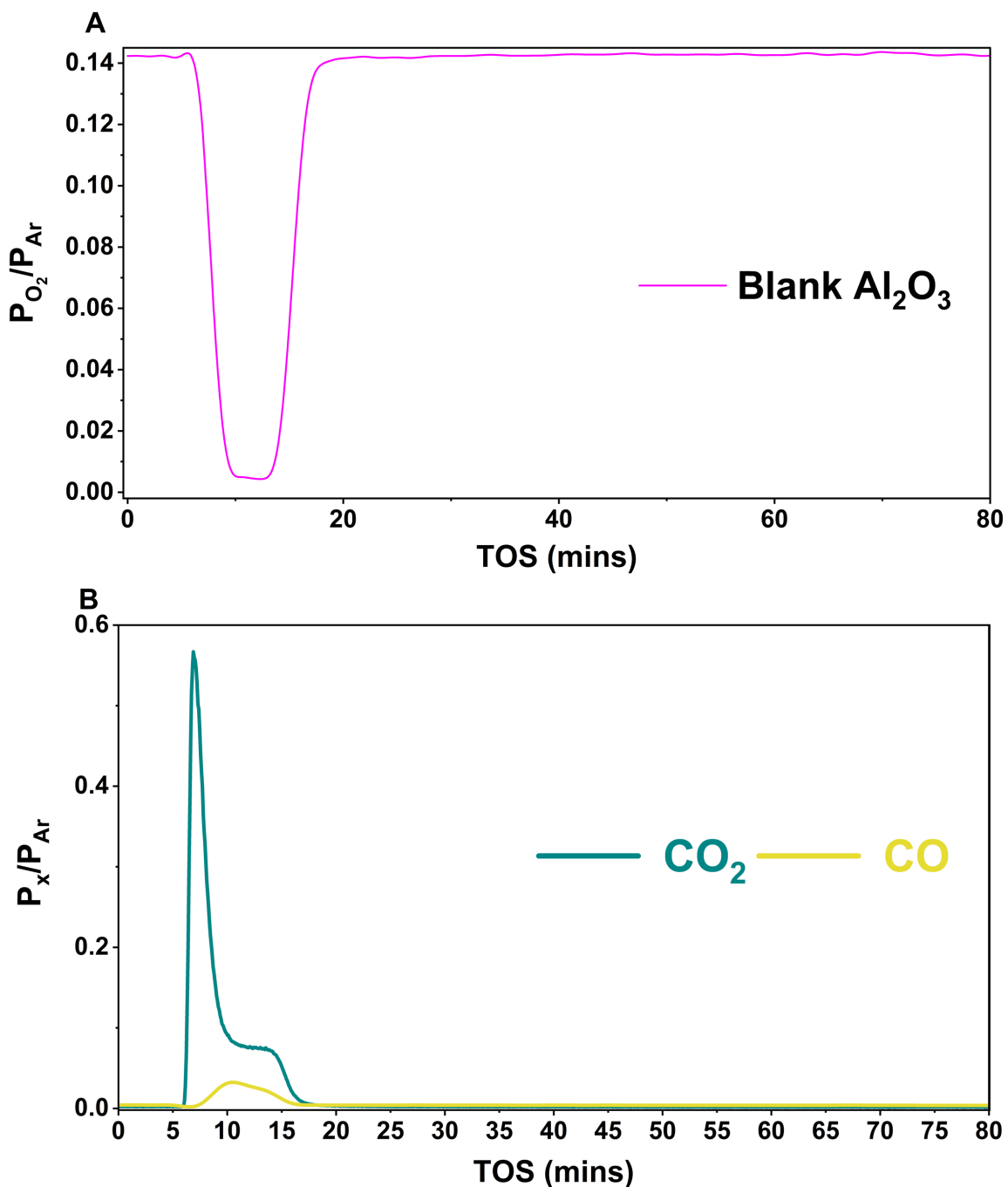


Fig. S-A.21 | Coke formation analysis on 3 g Al_2O_3 spheres with 0.28 g glass wool. **A)** The spheres are oxidized at 0.14 atm partial pressure of oxygen in argon at a temperature of 600 °C. **B)** Product partial pressures as a function of time throughout the oxidation

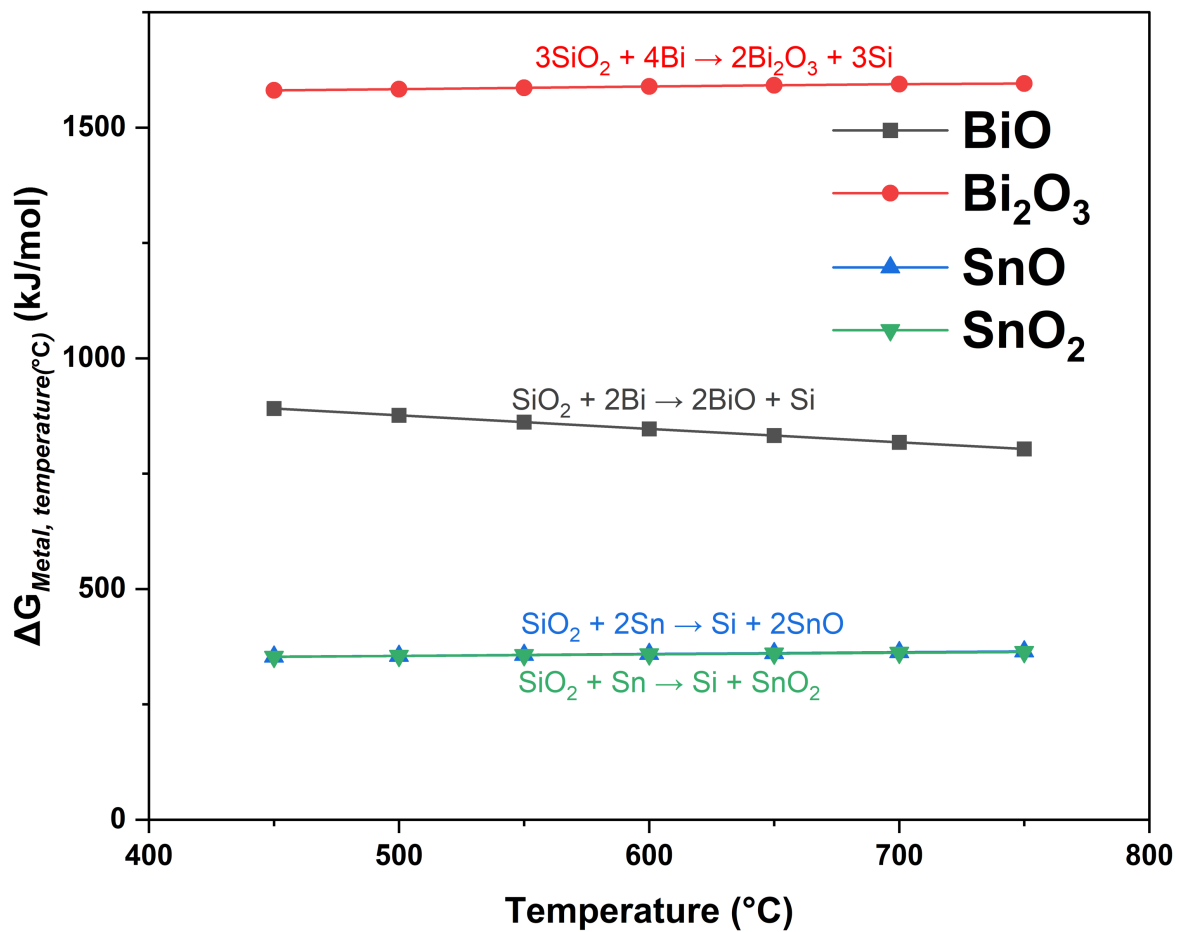


Figure S-A.22 | Summary of thermodynamic properties for SiO₂ oxidation with Bi and Sn. Note: Oxidation to all oxide intermediates are considered for both Bi and Sn

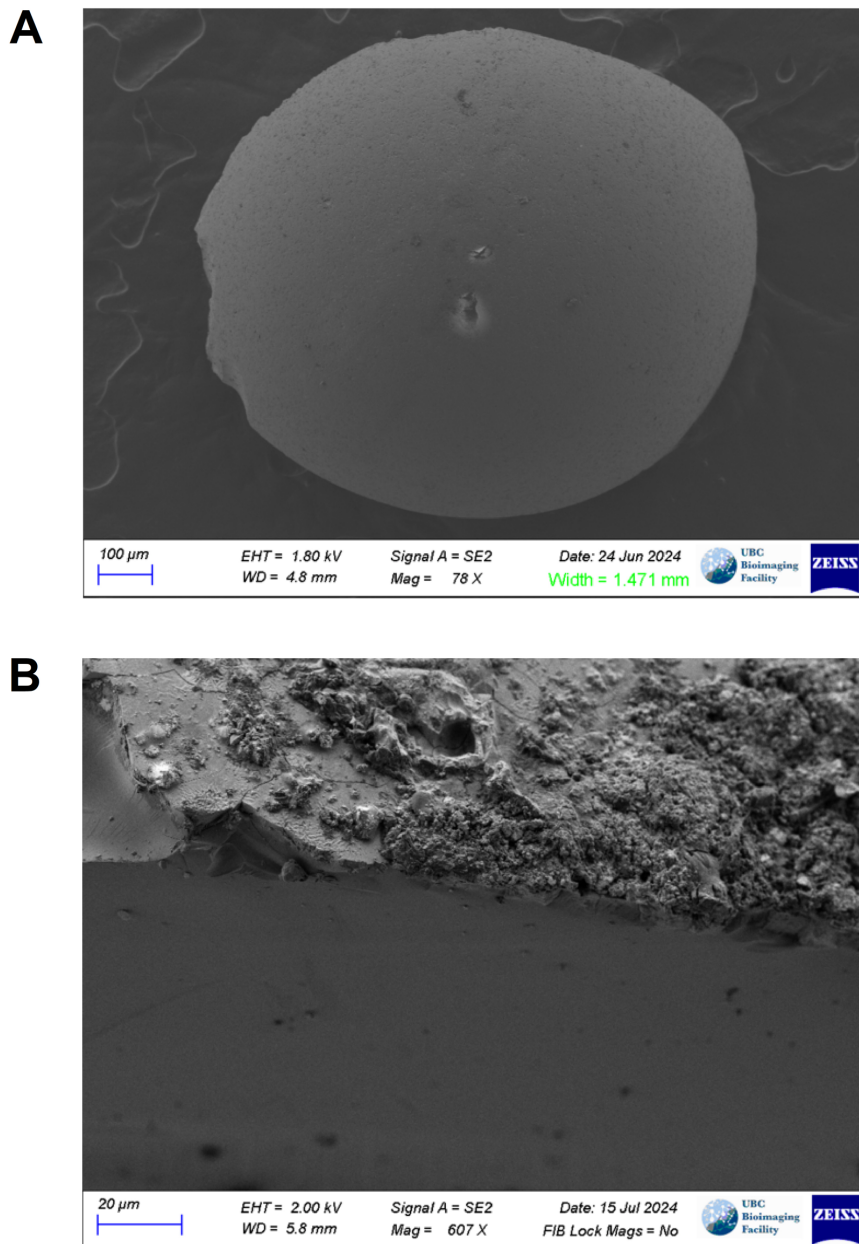


Fig. S-A.23 | SEM images of cracked 50-50 mol% Bi-Sn after catalysis. A) Cracked borosilicate bead and **B)** cracked 50-50 mol% Bi-Sn alloy after ODH catalysis with C_3H_8 at 0.125 atm partial pressure of propane in argon (1:8 C_3H_8 :Ar) at 600 °C. Note: 1 mm catalysts are fractured to approximately $\frac{1}{4}$ to $\frac{1}{2}$ their original size

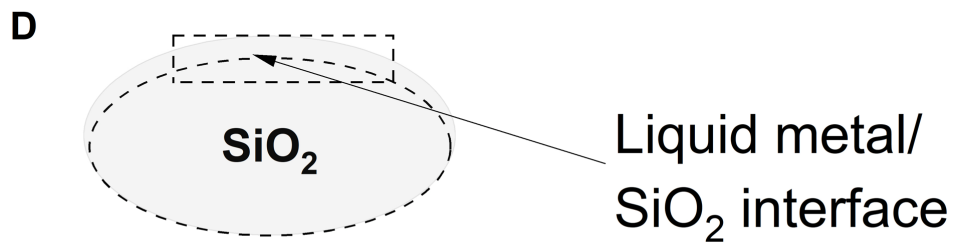
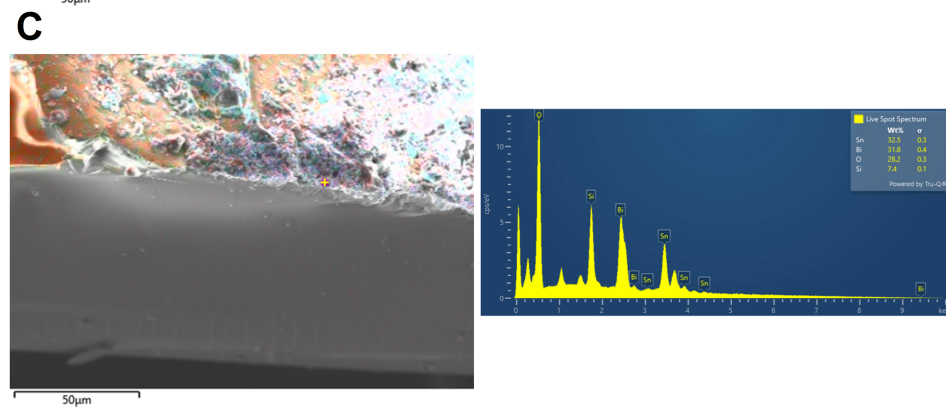
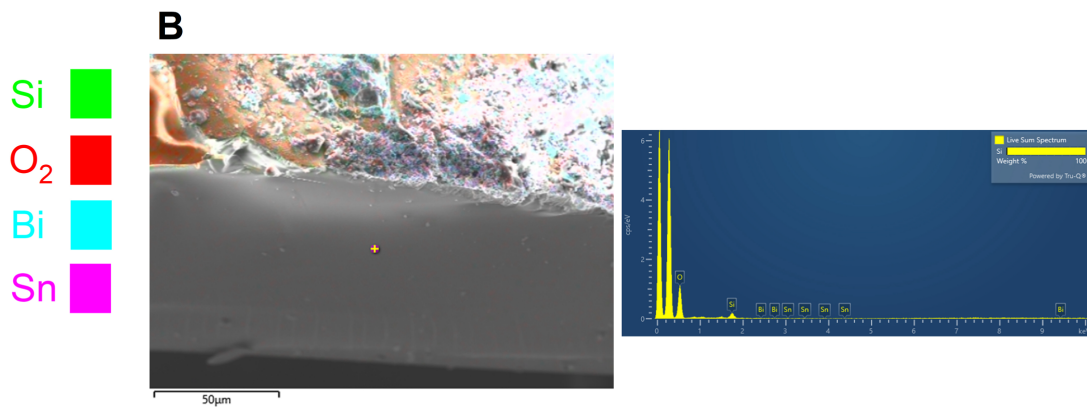
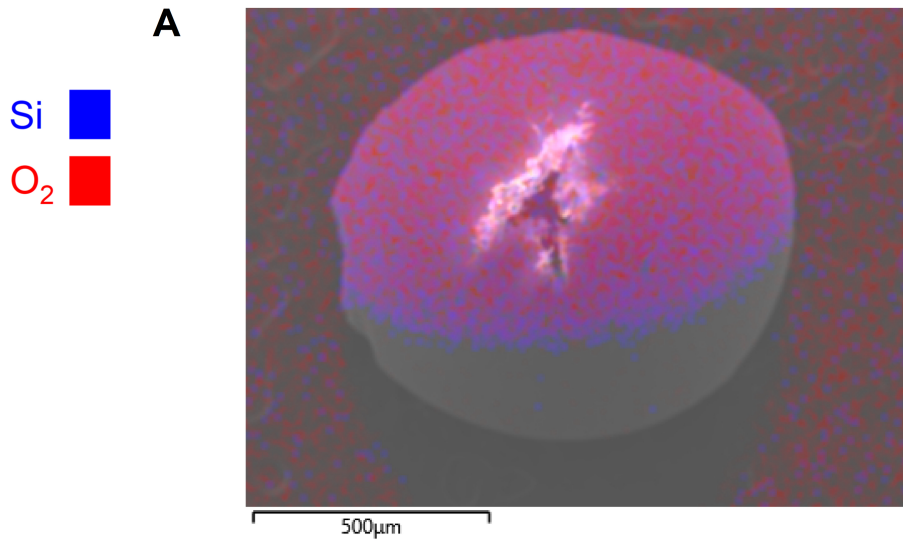


Fig. S-A.24 | Elemental mapping images of the supported 50-50 mol% Bi-Sn alloy after catalysis. **A)** Cracked borosilicate bead, **B)** cracked 50-50 mol% Bi-Sn alloy after ODH catalysis mapping the inner SiO₂ part, **C)** cracked 50-50 mol% Bi-Sn alloy after ODH catalysis mapping the immediate liquid metal/SiO₂ interface, and **D)** schematic of the region of analysis for **C**. Note: a 0.125 atm partial pressure of propane in argon (1:8 C₃H₈:Ar) is employed at 600 °C for **B** and **C**

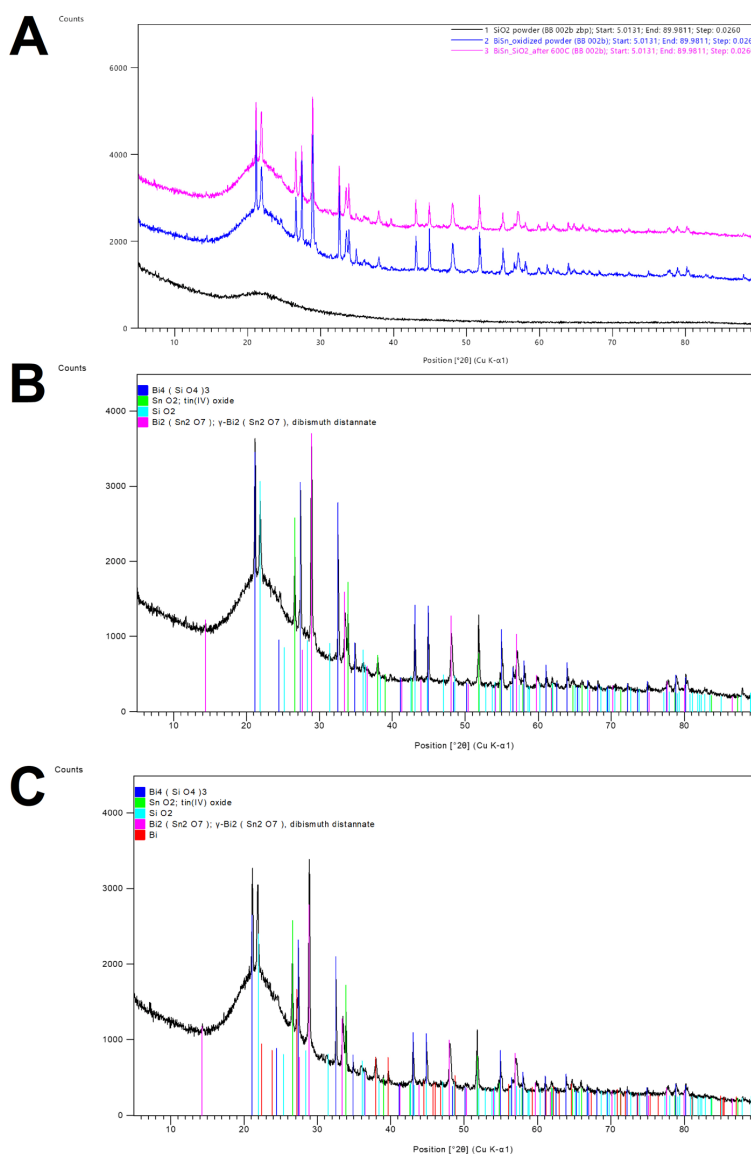


Fig. S-A.25 | Powder XRD images of the supported 50-50 mol% Bi-Sn alloy after oxidation and catalysis. **A)** XRD spectrum for a borosilicate bead, a 50-50 mol% Bi-Sn alloy after oxidation at 0.14 atm partial pressure of oxygen in argon (1:7 O₂:Ar) at 600

°C, and a 50-50 mol% Bi-Sn alloy after ODH catalysis with C₃H₈ at 0.125 atm partial pressure of propane in argon (1:8 C₃H₈:Ar) at 600 °C. **B)** Phase identification of spectrum 2 in **A**. **C)** Phase identification of spectrum 3 in **A**

Instrument Type	Malvern-Panalytical Empyrean 3 (Program 002b)
Tube	Cu LFF HR @ 45kV, 40mA
Incident Beam Optics	iCore
Divergence Slit	Fixed, 1/4°
Masks	14mm primary / 6mm secondary
Soller Slits	0.03rad
Filtration	Bragg-Brentano ^{HD} (BBHD mirror)
Sample Stage	Reflection/Transmission spinner – spinning on
Accessory	Sample Changer
Diffracted Beam Optics	dCore
Soller Slits	0.04rad
Anti-scatter slit	Fixed, 1/4°
Collimator	none
Detector	PIXcel ^{3D} in 1D mode
Configuration	Bragg-Brentano
Sample	<ul style="list-style-type: none"> • Powder is ground with a mortar and pestle which is thereafter packed in a shallow well of a zero-background plate

Table S-A.1 | Specifications of the powder XRD instrument in the UBC Chemistry department

Methods

Molten alloy preparation and overall experimentation procedure

The bulk metals for most of the screening experiments were procured from Sigma-Aldrich in powder form. The powdered metals were melted in a 0.503 cm² quartz crucible cup inserted into the custom surface reactor in which all screening experimentation occurred. Quartz was used as the reactor material for the custom screening reactor, the fixed-bed reactor, and the crucible cups. These had a glass transition temperature of 1200 °C and a melting point of 1685 °C. High purity pertinent gases, procured from Linde Canada Inc., were delivered to the system through SLA 5800 series Brooks[®] Instrument mass flow controllers from their respective cylinders. A Brooks[®] Instrument 0254 box was used to control the associated flow rates to the system. Moreover, an Omega pressure transducer and a thermocouple was included in the setup. A Lindberg/Blue M[™] furnace heated the custom surface reactor to the required temperatures; the outlet stream was wrapped in tape and heated to 120 °C to remove any water. All products were measured in a 200 amu residual gas analyzer from Stanford Research Systems.

The experimental procedures for the supported catalytic experiments were conducted using a tailored quartz u-tube reactor with a fixed-bed configuration. The solid borosilicate beads, used as the catalytic support material in the reactor, were obtained from Sigma-Aldrich. The borosilicate beads had a glass transition temperature of 547.5 °C and melting point of 1648 °C. We utilized quartz wool for experiments conducted at 650 °C and higher. Quartz wool was sourced from Thermo Fisher Scientific. It had a fine texture with a 4-micron specification and was used without any prior chemical treatment. The beads were selected for their lack of porosity and their size (1 mm diameter), which was designed to prevent the formation of excessive fines. The dimensionality analysis, particularly the Length to Diameter ($\frac{L}{D}$) ratio, yielded a mesh size of 12–20 for the borosilicate beads. This range was deliberately chosen to maintain a desirable pressure drop across the catalytic bed and to minimize axial dispersion, thereby targeting the enhancement of the overall reactor performance. The glass wool, utilized as the bed support within the reactor, was also purchased from Sigma-Aldrich and was placed exactly 22 cm from the top of the fixed-bed reactor. This measure was undertaken to ascertain consistent positioning of the catalytically active liquid melt throughout the course of the experiments. Glass wool, with an accurately measured mass of

0.28 g, was employed for this purpose. A proportion of the total weight between 22.51 and 22.6 wt% consisted of the respective metal which was supported on 3 g of borosilicate beads (Figs. S-A.3 and S-A.4). For a holistic overview and deliberation on the synthesis of the supported liquid melt, refer to Section 2.3 (Figs. S-A.3 and S-A.4). For our additional support experiments, alumina spheres (1-2 mm) were purchased from American Elements.

The reactant gases, employing a split-feed mechanism, flow through SLA 5800 series Brooks[®] Instrument mass flow controllers from their respective cylinders (Linde Canada Inc.). A Brooks[®] Instrument 0260 box was used to manipulate the associated flow rates to the system. At optimal operating conditions, the oxidation reaction was initiated over the surface of the liquid metal at a ratio of 1:7 sccm O₂:Ar. Thereafter, the reduction reaction, ODH in the presence of a soft oxidant, was undertaken at a ratio of 1:8 sccm C₃H₈:Ar. A custom 10 A furnace from the Mellen Company heated the fixed-bed reactor to the required temperature; a vertical stand was used to hold the furnace in place. The products and byproducts of the associated reactions flow out of the fixed-bed reactor system from the other end. Notably, the outlet stream was also wrapped in tape and heated to 130 °C to eliminate the residual and persistent generation of water. The products and reactants were measured in a 100 amu residual gas analyzer (UGA 100) from Stanford Research Systems. Additionally, the setup was executed in a vented enclosure, and the inlet and outlet streams were continuously monitored via separate ports connected to the UGA 100. A Multiple Gas #5 8610C Gas Chromatograph was procured from SRI Instruments and was tailored for both dehydrogenation reactions by Majd Tabbara. Namely, the columns were altered such that two 6' Haysep D columns were aligned in series closing off the 3' MoleSieve 5A column whilst retaining the 18' Haysep D column from valve 1 port 5. An in-series configuration was adopted where the gas of interest was directed through the aforementioned custom column configuration into the Thermal Conductivity Detector (TCD) followed by the Flame Ionization Detector (FID). This allowed for the detection of all gases as individual peaks on the chromatograms, except for the overlapping peak of CO and Ar which was computed through quantitative deconvolution.

Criterion for plug flow operation

In experiments where supported molten metals were used, borosilicate was used as the support material. In order to have plug flow, the reactor tube inner diameter (D_t) was 1.1 cm, the

borosilicate particle diameter (d_p) was 0.1 cm, resulting in $\frac{D_t}{d_p} = 11^{1,2}$.

Reactor performance evaluation metrics

Note: all selectivities are based on the gaseous products analyzed within the mass spectrometer.

$$C_3H_8 \text{ Conversion (\%)} = \left(\frac{\frac{P_{C_3H_8in}}{P_{Ar}} - \frac{P_{C_3H_8out}}{P_{Ar}}}{\frac{P_{C_3H_8in}}{P_{Ar}}} \right) * 100\%$$

$$O_2 \text{ Conversion (\%)} = \left(\frac{\frac{P_{O_2in}}{P_{Ar}} - \frac{P_{O_2out}}{P_{Ar}}}{\frac{P_{O_2in}}{P_{Ar}}} \right) * 100\%$$

$$\text{Product Yields (\%)} = \left(\frac{n_C \text{ product} * \frac{P_{product}}{P_{Ar}}}{n_C C_3H_8 * \frac{P_{C_3H_8in}}{P_{Ar}}} \right) * 100\%$$

$n_C \text{ species } i = \text{number of carbon atoms in species } i$

$$\text{Product Selectivities (\%)} = \left(\frac{\text{Product Yield}}{C_3H_8 \text{ Conversion}} \right) * 100\%$$

References

1. C. Chu and K. Ng, *AIChE Journal*, 1989, **35**, 148–158.
2. G. Ertl, H. Knözinger and J. Weitkamp, *Handbook of Heterogeneous Catalysis*, VCH Weinheim, 1997.